

Automatic code generator for higher order integrators

Asif Mushtaq^a, Kåre Olaussen^b

^a*Institutt for matematiske fag, NTNU, N-7491 TRONDHEIM, Norway*

^b*Institutt for fysikk, NTNU, N-7491 TRONDHEIM, Norway*

Abstract

Some explicit algorithms for higher order symplectic integration of a large class of Hamilton's equations have recently been discussed by Mushtaq *et. al.* Here we present a Python program for automatic numerical implementation of these algorithms for a given Hamiltonian, both for double precision and multiprecision computations. We provide examples of how to use this program, and illustrate behaviour of both the code generator and the generated solver module(s).

Keywords: Splitting methods, Modified integrators, Higher order methods, Automatic code generation

2010 MSC: 33F05, 37M15, 46N40, 65P10, 74S30

PROGRAM SUMMARY

Manuscript Title: Automatic code generator for higher order integrators.

Authors: Asif Mushtaq, Kåre Olaussen.

Program Title: HOMsPy: Higher Order (Symplectic) Methods in Python

Journal Reference:

Catalogue identifier:

Licensing provisions: None.

Programming language: Python 2.7.

Computer: PC's or higher performance computers.

Operating system: Linux, MacOS, MSWindows.

RAM: Kilobytes to a several gigabytes (problem dependent).

Number of processors used: 1

Keywords: Splitting methods, Modified integrators, Higher order methods, Automatic code generation.

Classification: 4.3 Differential equations, 5 Computer Algebra.

External routines/libraries: SymPy library [1] for generating the code. NumPy library [2], and optionally mpmath [3] library for running the generated code. The matplotlib [4] library for plotting results.

Nature of problem: We have developed algorithms [5] for numerical solution of Hamilton's

Email addresses: Asif.Mushtaq@math.ntnu.no (Asif Mushtaq), Kare.Olaussen@ntnu.no (Kåre Olaussen)

equations,

$$\dot{q}^a = \frac{\partial H(\mathbf{q}, \mathbf{p})}{\partial p_a}, \quad \dot{p}_a = -\frac{\partial H(\mathbf{q}, \mathbf{p})}{\partial q^a}, \quad a = 1, \dots, \mathcal{N} \quad (1)$$

for Hamiltonians of the form

$$H(\mathbf{q}, \mathbf{p}) = T(\mathbf{p}) + V(\mathbf{q}) = \frac{1}{2} \mathbf{p}^T \mathbf{M} \mathbf{p} + V(\mathbf{q}), \quad (2)$$

with \mathbf{M} a symmetric positive definite matrix. The algorithms preserve the symplectic property of the time evolution exactly, and are of orders τ^N (for $2 \leq N \leq 8$) in the timestep τ . Although explicit, the algorithms are time-consuming and error-prone to implement numerically by hand, in particular for larger N .

Solution method: We use computer algebra to perform all analytic calculations required for a specific model, and to generate the Python code for numerical solution of this model, including example programs using that code.

Restrictions: In our implementation the mass matrix is assumed to be equal to the unit matrix, and $V(\mathbf{q})$ must be sufficiently differentiable.

Running time: Subseconds to eons (problem dependent). See discussion in the main article.

Program: Python program can be provided on demand from authors.

References

- [1] *SymPy Development Team*, <http://sympy.org/>
- [2] *NumPy Developers*, <http://numpy.org/>
- [3] Fredrik Johansson *et. al.*, *Python library for arbitrary-precision floating-point arithmetic*, <http://code.google.com/p/mpmath/> (2010)
- [4] J.D. Hunter, *Matplotlib: A 2D graphics environment*, Computing in Science & Engineering **9**, 90–95 (2007)
- [5] A. Mushtaq, A. Kværnø, K. Olaussen, *Higher order Geometric Integrators for a class of Hamiltonian systems*, International Journal of Geometric Methods in Modern Physics, vol 11, no. 1 (2014), 1450009-1–1450009-20. DOI: 10.1142/S0219887814500091. arXiv.org:1301.7736

1. Introduction

The Hamilton equations of motion (1) play an important role in physics and mathematics. They often require numerical methods for solution [1, 2, 3]. A well-behaved class of such methods are the *symplectic solvers*, which preserve symplecticity of the time evolution exactly. One simple way to construct a symplectic solver is to split the time evolutions into *kicks*,

$$\dot{q}^a = 0, \quad \dot{p}_a = -\frac{\partial V(\mathbf{q})}{\partial q^a}, \quad (3)$$

which is straightforward to integrate to give

$$q^a(t + \tau) = q^a(t), \quad (4)$$

$$p_a(t + \tau) = p_a(t) - \tau \frac{\partial V(\mathbf{q}(t), \mathbf{p}(t))}{\partial q^a}, \quad (5)$$

followed by *moves*,

$$\dot{q}^a = \frac{\partial T(\mathbf{p})}{\partial p_a} = \sum_b M^{ab} p_b, \quad \dot{p}_a = 0, \quad (6)$$

which integrates to

$$q^a(t + \tau) = q^a(t) + \tau \sum_b M^{ab} p_b(t + \tau),$$

$$p_a(t + \tau) = p_a(t) - \tau \frac{\partial V(\mathbf{q}(t), \mathbf{p}(t))}{\partial q^a}.$$

This scheme was already introduced by Newton [4] (as more accessible explained by Feynman [5]). A symmetric scheme is to make a *kick* of size $\frac{1}{2}\tau$, a *move* of size τ , and a *kick* of size $\frac{1}{2}\tau$ (and repeating). This is often referred to as the Störmer-Verlet method [6, 7]; it has a local error of order τ^3 . The solution provided by this method can be viewed as the exact solution of a slightly different Hamiltonian system, with a Hamiltonian H_{SV} which differ from (2) by an amount proportional to τ^2 . For this reason the scheme respects long-time conservation of energy to order τ^2 . It will also exactly preserve conservation laws due to Nöther symmetries which are common to $T(\mathbf{p}) = \frac{1}{2}\mathbf{p}^T \mathbf{M} \mathbf{p}$ and $V(\mathbf{q})$, like momentum and angular momentum which are often preserved in physical models [8].

Recently Mushtaq *et. al.* [9, 10] proposed some higher order extensions of the Störmer-Verlet scheme. These extensions are also based on the *kick-move-kick* idea, only with modified Hamiltonians,

$$H_1 \equiv T_{\text{eff}} = \frac{1}{2}\mathbf{p}^T \mathbf{M} \mathbf{p} + \sum_{k \geq 1} T_{2k}(\mathbf{q}, \mathbf{p}), \quad (7a)$$

$$H_2 \equiv V_{\text{eff}} = V(\mathbf{q}) + \sum_{k \geq 1} V_{2k}(\mathbf{q}), \quad (7b)$$

where T_{2k} and V_{2k} are proportional to τ^{2k} . I.e., the proposal is to replace $V(\mathbf{q})$ in equation (3) by $V_{\text{eff}}(\mathbf{q})$, and $T(\mathbf{p})$ in equation (6) by $T_{\text{eff}}(\mathbf{q}, \mathbf{p})$. The goal is to construct V_{eff} and T_{eff} such that the combined *kick-move-kick* process corresponds to an evolution by a Hamiltonian H_{eff} which lies closer to the Hamiltonian H of equation (2). The difference being of order τ^{2N+2} when summing terms to $k = N$ in equations (7).

One problem with this approach is that T_{eff} in general will depend on both \mathbf{q} and \mathbf{p} ; hence the *move*-steps of equation (6) can no longer be integrated explicitly. To overcome this problem we introduce a generating function [3]

$$G(\mathbf{q}, \mathbf{P}; \tau) = \sum_{0 \leq k \leq N} G_k(\mathbf{q}, \mathbf{P}) \tau^k \quad (8)$$

such that the transformation $(\mathbf{q}, \mathbf{p}) \rightarrow (\mathbf{Q}, \mathbf{P})$ defined by

$$p_a = \frac{\partial G}{\partial q^a}, \quad (9a)$$

$$Q^a = \frac{\partial G}{\partial P_a}, \quad (9b)$$

preserves the symplectic structure exactly, and reproduce the time evolution generated by T_{eff} to order τ^N . Here Q^a is shorthand for $q^a(t + \tau)$, and P_a shorthand for $p_a(t + \tau)$. Equation (9a) is implicit and in general nonlinear, but the nonlinearity is of order τ^3 (hence small for practical values of τ). In the numerical code we solve (9a) by straightforward iteration (typically two to four iterations in the cases we have investigated).

The rest of this paper is organized as follows: In section 2 we introduce compact notation in which we present the general explicit expressions for $T_{\text{eff}}(\mathbf{q}, \mathbf{p})$, $V_{\text{eff}}(\mathbf{q})$, and $G(\mathbf{q}, \mathbf{Q})$. Because of their compactness these expressions are straightforward to implement in SymPy.

In section 3 we provide examples of how to use the code generator on specific problems. This process proceeds through two stages: (i) By providing the potential $V(\mathbf{q})$ (possibly depending on extra parameters) code for solving the resulting Hamilton's equations (the solver module) is generated, and (ii) this solver module is used to analyse the model. The last stage must of course be implemented by the user, but an example program which explicitly demonstrates how the solver module can be used is also generated during the first stage.

The examples given in subsections 3.1 (Vibrating beam) and 3.2 (One-parameter family of quartic anharmonic oscillators) have known exact solutions; this makes it easy to check whether the algorithms behave like expected with respect to accuracy. The example in subsection 3.3 (two-dimensional pendulum) demonstrates that the program can handle nonpolynomial functions, and that it generates code which preserves angular momentum exactly.

In section 4 we consider a collection of many coupled quartic oscillators. This is intended as a stress-test of the code, investigating how it behaves with respect to precision as well as time and memory use for larger and more complex models. Test of both of the code-generating process, and of the solver modules generated. We find that the latter continue to behave as expected with respect to accuracy, but that there is room for improvement in the area of time and memory efficiency, in particular for large structured systems.

In section 5 we present the organization of our code generating program itself, including diagrammatic representations of its structure. We finally summarize our experiences in section 6.

2. Explicit expressions

Compact explicit expressions for the terms of order τ^N for $N \in \{2, 4, 6\}$ in equations (7) were given in [9, 10]. With the notation

$$\partial_a \equiv \frac{\partial}{\partial q^a}, \quad \partial^a \equiv M^{ab} \partial_b, \quad p^a \equiv M^{ab} p_b, \quad D \equiv p_a \partial^a, \quad \bar{D} \equiv (\partial_a V) \partial^a, \quad (10)$$

where the *Einstein summation convention*¹ is employed, they are

$$T_2 = -\frac{1}{12}D^2V\tau^2, \quad (11a)$$

$$T_4 = \frac{1}{720}(D^4 - 9\bar{D}D^2 + 3D\bar{D})V\tau^4, \quad (11b)$$

$$T_6 = -\frac{1}{60480}(2D^6 - 40\bar{D}D^4 + 46D\bar{D}D^3 - 15D^2\bar{D}D^2 + 54\bar{D}^2D^2 - 9\bar{D}D\bar{D}D - 42D\bar{D}^2D + 12D^2\bar{D}^2)V\tau^6 \quad (11c)$$

$$V_2 = \frac{1}{24}\bar{D}V\tau^2, \quad (11d)$$

$$V_4 = \frac{1}{480}\bar{D}^2V\tau^4, \quad (11e)$$

$$V_6 = \frac{1}{161280}(17\bar{D}^3 - 10\bar{D}_3)V\tau^6. \quad (11f)$$

In the last line we have introduced

$$\bar{D}_3 \equiv (\partial_a V)(\partial_b V)(\partial_c V)\partial^a\partial^b\partial^c. \quad (12)$$

By introducing the operator $\mathcal{D} = P^a\partial_a$ the explicit expressions for the coefficients G_k can be written

$$G_0 = q^a P_a, \quad (13a)$$

$$G_1 = \frac{1}{2}P^a P_a, \quad (13b)$$

$$G_2 = 0, \quad (13c)$$

$$G_3 = -\frac{1}{12}\mathcal{D}^2V, \quad (13d)$$

$$G_4 = -\frac{1}{24}\mathcal{D}^3V, \quad (13e)$$

$$G_5 = -\frac{1}{240}(3\mathcal{D}^4 + 3\bar{D}\mathcal{D}^2 - \mathcal{D}\bar{D}\mathcal{D})V, \quad (13f)$$

$$G_6 = -\frac{1}{720}(2\mathcal{D}^5 + 8\bar{D}\mathcal{D}^3 - 5\mathcal{D}\bar{D}\mathcal{D}^2)V, \quad (13g)$$

$$G_7 = -\frac{1}{20160}(10\mathcal{D}^6 + 10\bar{D}\mathcal{D}^4 + 90\mathcal{D}\bar{D}\mathcal{D}^3 - 75\mathcal{D}^2\bar{D}\mathcal{D}^2 + 18\bar{D}^2\mathcal{D}^2 - 3\bar{D}\mathcal{D}\bar{D}\mathcal{D} - 14\mathcal{D}\bar{D}^2\mathcal{D} + 4\mathcal{D}^2\bar{D}^2)V, \quad (13h)$$

$$G_8 = -\frac{1}{40320}(3\mathcal{D}^7 - 87\bar{D}\mathcal{D}^5 + 231\mathcal{D}\bar{D}\mathcal{D}^4 - 133\mathcal{D}^2\bar{D}\mathcal{D}^3 + 63\bar{D}^2\mathcal{D}^3 - 3\mathcal{D}\bar{D}^2\mathcal{D}^2 - 21\mathcal{D}^2\bar{D}^2\mathcal{D} + 4\mathcal{D}^3\bar{D}^2 - 63\bar{D}\mathcal{D}\bar{D}\mathcal{D}^2 + 25\mathcal{D}\bar{D}\mathcal{D}\bar{D}\mathcal{D})V. \quad (13i)$$

¹An index which occur twice, once in lower position and once in upper position, are implicitly summed over all available values. I.e., $M^{ab}\partial_b \equiv \sum_b M^{ab}\partial_b$ (we generally use the matrix M to rise an index from lower to upper position).

The equations (11,13), when used in equations (3,9), define the *kick-move-kick* scheme for a general potential V . If one uses all the listed terms the local error becomes of order τ^9 , and the scheme will respect long-time conservation of energy to order τ^8 .

However, explicit implementation of the numerical code for a specific potential is rather laborious and error-prone to do by hand, since the repeated differentiations (with respect to many variables) and multiplications by lengthy expressions are usually involved. We have therefore written a code-generating program in SymPy, which takes a given potential V as input, perform all the necessary algebra symbolically, and automatically constructs a Python module for solving one full *kick-move-kick* timestep. It also writes a Python program example using the module; this example may serve as a template for larger applications.

3. Examples of code generation

The submitted code includes a file `makeExamples.py`, with various examples which demonstrate how the code generator can be used. We go through these examples in this section; they also provide some illustrations of how the integrators perform in practical use.

3.1. Vibrating beam

A simple model for a vibrating beam is defined by the Hamiltonian

$$H = \frac{1}{2}p^2 - \frac{1}{2}q^2 + \frac{1}{4}q^4. \quad (14)$$

A Python code snippet which generates a numerical solver for this problem is the following:

Creating a module for solving a vibrating beam

```
1 def makeVibratingBeam():
2     # Choose names for coordinate and momentum
3     q, p = sympy.symbols(['q', 'p'])
4     qvars = [q]; pvars = [p]
5     # Define the potential in terms of the coordinate
6     V = -q*q/2 + q**4/4
7     # Create code for a double-precision solver
8     kimoki.makeModules('VibratingBeam', V, qvars, pvars)
```

Line 8 generates the files `VibratingBeam.py` and `runVibratingBeam.py`. The file `VibratingBeam.py` contains the general double precision solver module for this problem. A simple use of it in an interactive session is illustrated below:

Interactive use of the solver module

```
1 >>> from __future__ import division
2 >>> from VibratingBeam import *
3 >>> z = numpy.array([1/2, 5/4])
4 >>> kiMoKi(z); print z
```

```

5 [ 0.62690658  1.28822851]
6 >>> kiMoKi(z); print z
7 [ 0.75756578  1.32399846]

```

Here $z = [q, p]$ is a NumPy array containing the current state of the solution. Each call of `kiMoKi` updates this state (data from previous timesteps are not kept).

The file `runVibratingBeam.py` is a small example program demonstrating basic use of `VibratingBeam.py`. A code snippet illustrating some essential steps is:

Time evolution of a vibrating beam

```

1 # Select your preferred number of timesteps, order and timestep
2   nMax = 161
3   VibratingBeam.order = 8; VibratingBeam.tau = 1/10
4   z = numpy.array([1/2, 5/4]) # Initial condition
5   for n in xrange(nMax):
6       VibratingBeam.kiMoKi(z) # Integrate one full timestep

```

The equation is integrated in line 6. The complete code in `runVibratingBeam.py` is an extension of this snippet. The initial condition is generated at random, and saved for possible reuse. Also the complete solution is saved to a (temporary) file for further processing, together with the parameters `tau`, `order`, and `nMax`. By running the file `runVibratingBeam.py` a single solution is first generated and afterwards displayed in a plot. The plot is also saved in the file `VibratingBeam_Soln.png`. This plot will look similar to Figure 1.

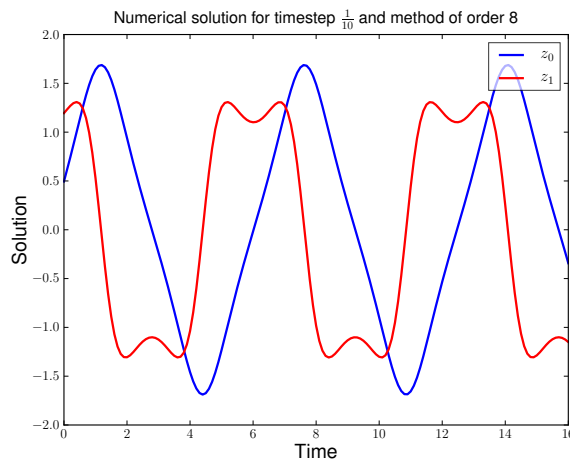


Figure 1: Example solution of a vibrating beam with random initial conditions. Here z_0 denotes the position q , and z_1 the momentum p .

To give some impression of the quality of the generated solution, and how this depends on the timestep and order of the integrator, the example runfile also make a set

of runs with the same initial condition, but various values of τ , order , and nMax . A simple quality measure, which is straightforward to implement in general, is how well the initial energy is preserved as time increases. This quantity is plotted, with the plot first displayed and next saved in the file `VibratingBeam_EgyErr.png`. The plot will look similar to Figure 2. If one prefers to save the plots as .pdf-files the code

```
#import matplotlib; matplotlib.use('PDF') # Uncomment to ...
```

on line 17 of the example runfile must be uncommented (then the plot will most likely not be displayed on screen). During the run process solution data is saved to several .pkl-files; these are normally removed after the data has been plotted. To keep this data the code

```
os.remove(filename) # Comment out to keep datafile
```

on lines 108 and/or 202 of the example runfile must be commented out.

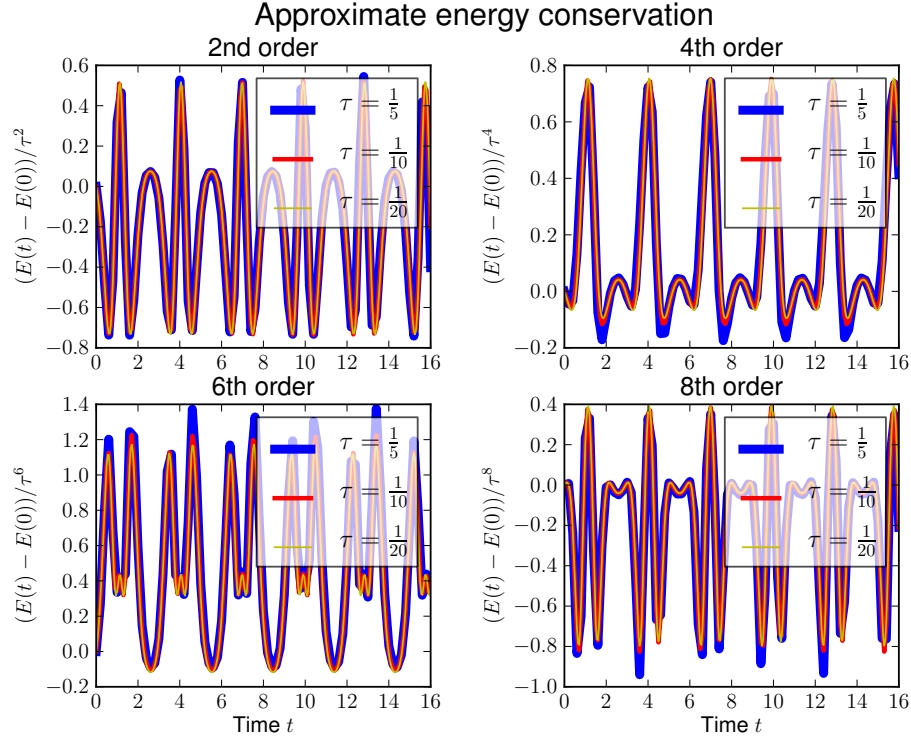


Figure 2: Example of how well energy is conserved for integrators of various orders N , and how the energy errors scale as expected with the timestep τ . The error decreases like τ^N when τ decreases. In this case, with a periodic solution, there is also a periodic variation in the energy error.

As illustrated by Figure 2, and verified by all other cases we have investigated, the energy error scales like τ^N , where τ is the timestep and N is the order of the integrator.

N	$\tau = 0.2$	$\tau = 0.1$	$\tau = 0.05$
2	0.26	0.26	0.26
4	1.03	0.84	0.73
6	1.23	1.01	0.88
8	1.54	1.25	1.09

Table 1: Evaluation time per integration step in milliseconds, dependent on timestep τ and method order N . The higher order methods ($N > 2$) run faster for smaller τ because the iterative solution of (9a) requires fewer iterations, hence becomes faster. This example, like all others, have been run on a workstation equipped with two four-core Intel Xeon E5520 processors. The *ratio* between numbers like those above are probably more relevant than their absolute values.

The energy error does not grow with time, but varies in a periodic manner — following the periodicity of the generated solution. Note that the integration module, in this case `VibratingBeam`, contains a parameter `epsilon` which governs how accurate (9a) is solved. We have observed a systematic growth in the energy error when this parameter is chosen too large, thereby violating symplecticity (too much).

Another property of interest and importance is how the average time per integration step varies with the order of the method. The run example prints a measure of the computer time used. The results of this, for a longer run than the unmodified run example, are shown in Table 1. As can be seen, the penalty of using a higher order method is quite modest for a simple model like the vibrating beam, in particular when the timestep τ is small.

The exact solution of this problem can be expressed in terms of Jacobi elliptic functions, cf. equations (16) below. This allows direct comparison between the exact and the numerical solutions, as shown in Figure 3. The initial condition is chosen such that the energy is close to the critical energy, $E = 0$, where the solutions bifurcates from motion over the potential hill at $q = 0$ to motion in only one of the two potential wells. The exact solution moves over the potential hill. As can be seen, this is respected by the solutions of order $N = 6$ and 8, but not by the solutions of order $N = 2$ (Störmer-Verlet) and 4. This demonstrates that there may be cases where a higher order method, or an impractically small stepsize τ , is required to obtain even the qualitatively correct solution.

Up to the time t we have computed and plotted the solutions, the order $N = 8$ numerical solution cannot be visually distinguished from the exact one in this plot. A difference would become visible for sufficiently large t , because the two solutions have slightly different periods. The difference in periods is of order τ^8 for $N = 8$.

3.2. One-parameter family of quartic anharmonic oscillators

A generalization of the previous problem is the class of non-linear oscillators defined by the Hamiltonian

$$H = \frac{1}{2}p^2 + \frac{1}{2}\alpha q^2 + \frac{1}{4}q^4. \quad (15)$$

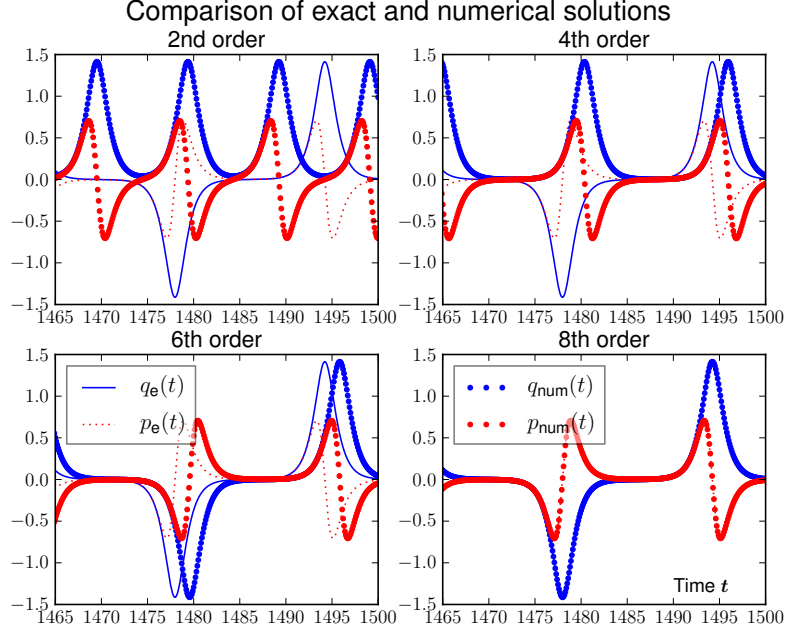


Figure 3: Comparison of the exact elliptic solution (16) with those found by our automatically generated numerical code, for the initial condition $q_0 = \sqrt{2} + 10^{-6}$ and $p_0 = 0$, with timestep $\tau = 10^{-1}$. The thick blue [red] lines show the numerical solutions for $q(t)$ [$p(t)$], the thin blue [red] lines show the exact solution for $q(t)$ [$p(t)$].

A one-parameter class of exact solutions to this problem can be expressed in terms of Jacobi elliptic functions [11],

$$q(t) = q_0 \operatorname{cn}(vt|k), \quad (16a)$$

$$p(t) = -q_0 v \operatorname{sn}(vt|k) \operatorname{dn}(vt|k). \quad (16b)$$

Here the initial conditions are $q(0) = q_0$, and $p(0) = 0$. The vibrating beam discussed in the previous subsection corresponds to the case of $\alpha = -1$. Equations (16) exhaust the set of solutions which have a maximum at $q_0 > 0$ (or a minimum at $q_0 < 0$). This condition imposes the restriction that $\alpha + q_0^2 \geq 0$. The parameters and energy of the solution are

$$v = (\alpha + q_0^2)^{1/2}, \quad k = 2^{-1/2} q_0 / v, \quad E = \frac{1}{2} \alpha q_0^2 + \frac{1}{4} q_0^4. \quad (17)$$

For $\alpha + \frac{1}{2} q_0^2 > 0$ the energy is positive, and $q(t)$ oscillates symmetrically around $q = 0$; for $\alpha + \frac{1}{2} q_0^2 < 0$ the energy is negative, and $q(t)$ oscillates in one of the two possible potential wells (depending on the sign of q_0). For $\alpha + q_0^2 < 0$ the solution has a minimum

at $q_0 > 0$ (or maximum at $q_0 < 0$).²

A code snippet for generating numerical solvers for this problem is the following

Solving a one-parameter class of anharmonic oscillators

```

1 def makeAnharmonicOscillator():
2     # Choose names for coordinate, momentum and parameter
3     q, p, alpha = sympy.symbols(['q', 'p', 'alpha'])
4     qvars = [q]; pvars = [p]; params = [alpha]
5     # Define potential in terms of coordinate and parameters
6     V = alpha*q**2/2 + q**4/4
7     # Code for double-precision and multiprecision computations
8     kimoki.makeModules('AnharmonicOscillator', V, qvars, pvars,
9                        PARAMS=params, MP=True, VERBOSE=True)

```

The code in line 8-9 shows that the makeModules function may take optional arguments: If the Hamiltonian depends on a list of parameters, this list must be assigned to the keyword PARAMS. If the MP keyword is set to True then two additional files are generated: In this case the files AnharmonicOscillatorMP.py, which is a solver module using multiprecision arithmetic, and runAnharmonicOscillatorMP.py, which is a runfile example using this multiprecision solver. When the VERBOSE keyword is set to True some information from the code generating process will be written to screen, mainly information about the time used to process the various stages. This may be of use when the code generation process takes a very long time, as will happen with complicated models.

²In which case the solution can be written

$$q(t) = q_0 \operatorname{nd}(vt, k), \quad p(t) = v q_0 k^2 \operatorname{sd}(vt, k) \operatorname{cd}(vt, k), \quad (18)$$

with $v = (-\alpha - q_0^2/2)^{1/2}$ and $k = v^{-1}(-\alpha - q_0^2)^{1/2}$. In (16) the modulus $k > 1$ when $\alpha + q_0^2/2 < 0$. An alternative expression, with $0 < k < 1$, is

$$q(t) = q_0 \operatorname{dn}(vt, k), \quad p(t) = -v q_0 \operatorname{sn}(vt, k) \operatorname{cn}(vt, k), \quad (19)$$

where $v = 2^{-1/2} q_0$ and $k = q_0^{-1} [2(\alpha + q_0^2)]^{1/2}$.

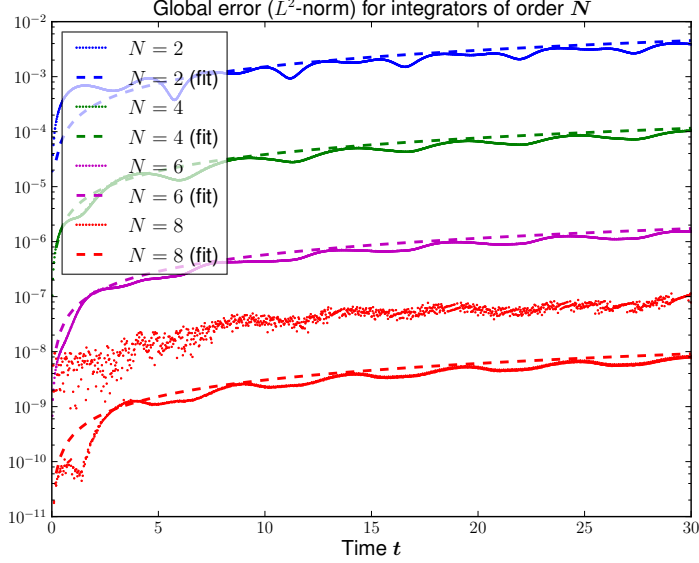


Figure 4: The global error (20) computed for integrators of various orders N , and stepsizes $\tau = \frac{1}{5}, \frac{1}{10}, \frac{1}{20}, \frac{1}{40}$. To check the τ^N -scaling the errors for the last three τ 's are multiplied by respectively $2^N, 4^N, 8^N$. The dashed lines are crude fits to equation (21) with C_N as the fitting parameters. The plot is not untypical, with the $N = 8$ result deviating from (21) for the smallest values of τ . This is a consequence of the finite accuracy of double precision calculations, not a failure of the $N = 8$ integrator.

To check the accuracy of the numerical solution in more detail, we have modified `runAnharmonicOscillator.py` to `analyseAnharmonicOscillator.py`, where the *global error*

$$\varepsilon(t) \equiv \|(q_{(e)}(t_m), p^{(e)}(t_m)) - (q_{(n)}^m, p_m^{(n)})\| \quad (20)$$

is computed (for random values of α and q_0), and plotted. Here the sub|super-script (e) labels the exact solution, and (n) the numerical one. One resulting plot, for parameters $\alpha = 0.13$ and $q_0 = 0.54$, is shown in Figure 4. In general, the global error fits well to the formula, cf. theorem 3.1 in the book [3],

$$\varepsilon(t) \equiv C_N \tau^N t, \quad (21)$$

where N is the order of the integrator, and C_N is independent of τ but depends on the parameters of the model, the initial conditions, and the norm $\|\cdot\|$ used in (20). We have used the L^2 norm in Figures 4 and 5.

It can be deduced from Figure 4 that to fully exploit the power of the higher order integrators one must go beyond double precision accuracy. We have therefore implemented an option (`MP=True`) for automatically generating multiprecision versions of the integrators and run examples. The file `analyseAnharmonicOscillatorMP.py` is an adaption of `runAnharmonicOscillatorMP.py` which computes the global error

to multiprecision accuracy. The result for $N = 8$ and various small values of τ (and the same parameters as in Figure 4) is shown in Figure 5.

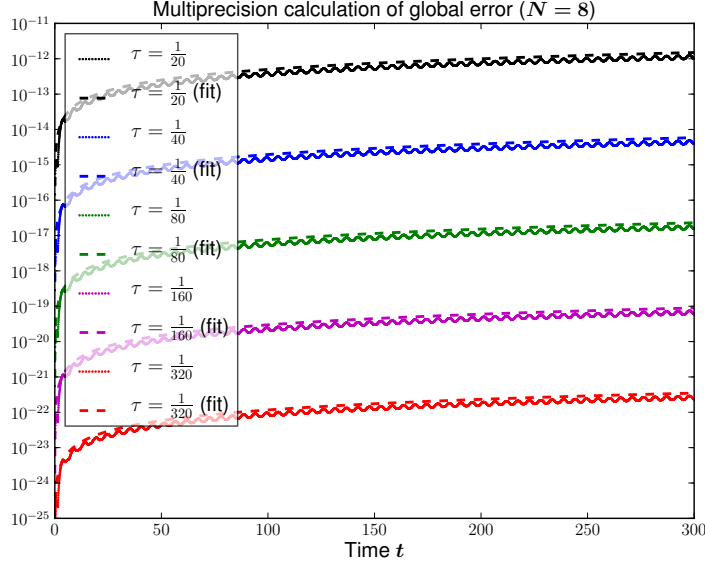


Figure 5: The global error (20) computed to 35 decimals precision for the $N = 8$ integrator, with stepsizes $\tau = \frac{1}{20}, \frac{1}{40}, \frac{1}{80}, \frac{1}{160}$, and $\frac{1}{320}$. The dashed lines correspond to equation (21), with C_8 fitted crudely to the $\tau = \frac{1}{20}$ data.

3.3. Two-dimensional pendulum

As a final example of this section we want to demonstrate that our program can handle non-polynomial potentials as well. Hence we consider the Hamiltonian for a slightly distorted³ version of a two-dimensional pendulum

$$H = \frac{1}{2} (p_0^2 + p_1^2) - \cos \left(\sqrt{q_0^2 + q_1^2} \right). \quad (22)$$

Here both the kinetic and potential energy is invariant under rotations; hence we expect the generated code to preserve angular momentum,

$$L(t) = [q_0(t)p_1(t) - q_1(t)p_0(t)], \quad (23)$$

exactly.

³The motion of a real pendulum is constrained to the surface of a sphere, which cannot be described by a constant mass matrix.

Solving a two-dimensional pendulum

```

1 def makeTwoDPendulum():
2     # Choose names for coordinate, momentum and parameter
3     q0, q1, p0, p1 = sympy.symbols(['q0', 'q1', 'p0', 'p1'])
4     qvars = [q0, q1]; pvars = [p0, p1]
5     # Define potential in terms of coordinate and parameters
6     V = -cos(sqrt(q0**2+q1**2))
7     # Code for multiprecision computation only
8     kimoki.makeModules('TwoDPendulum', V, qvars, pvars, DP=False,
9                       MP=True, MAXORDER=6, VERBOSE=True)

```

Here we demonstrated one additional optional argument of `makeModules`, `MAXORDER`, which can be used to restrict the maximum order of solvers being generated (6 in this example).

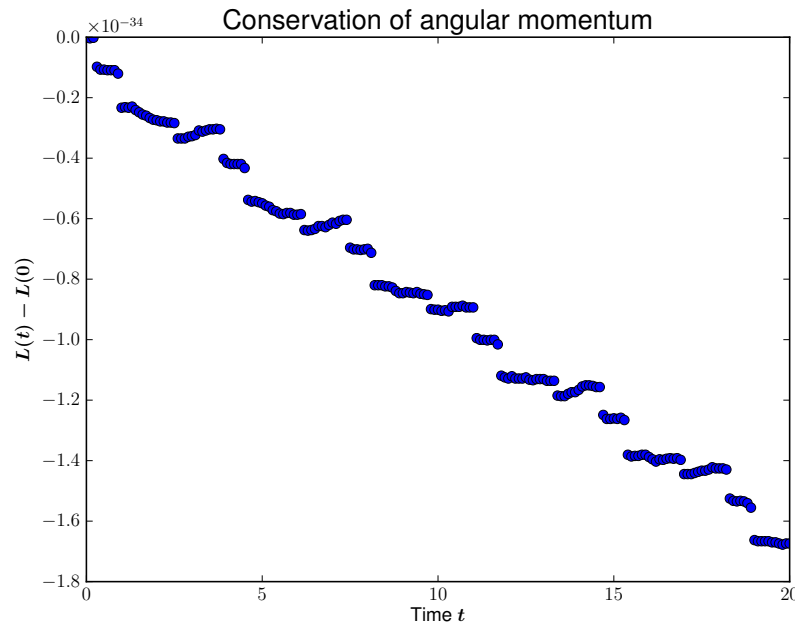


Figure 6: This figure demonstrates that our integration algorithm respects conservation of angular momentum exactly (within numerical accuracy). Here we have integrated Hamilton's equations with a timestep $\tau = 1/\text{mpf}(10)$ with an order = 6 multiprecision solver, using 35 decimal digits accuracy. Obviously, this figure only displays how roundoff errors are accumulated with time.

4. Analysis of many anharmonic oscillators

Consider a sum of Hamiltonians like (15),

$$H = \sum_{a=1}^{\mathcal{N}} \left[\frac{1}{2} P_a^2 + \frac{1}{2} \alpha_a (Q^a)^2 + \frac{1}{4} (Q^a)^4 \right]. \quad (24)$$

Since the corresponding Hamiltonian equations of motion decouple, the solution for each pair (Q^a, P_a) is given by expressions like (16). A direct numerical solution of this model would not provide any additional test of the integrators. However, if we make an orthogonal coordinate transformation,

$$Q^a = \sum_{j=1}^{\mathcal{N}} R_a^j q^j, \quad P_a = \sum_{j=1}^{\mathcal{N}} R_a^j p_j, \quad (25)$$

we obtain an expression

$$H = \frac{1}{2} \sum_{j=1}^{\mathcal{N}} p_j^2 + V(\mathbf{q}), \quad (26)$$

where $V(\mathbf{q})$ looks like a general polynomial potential in \mathcal{N} variables with quadratic and quartic terms. We expect the numerical algorithms to behave like the general case for this model, while the exact solution is known in the form

$$q_{(e)}^j = \sum_a R_a^j Q_{(e)}^a, \quad p_j^{(e)} = \sum_a R_a^j P_a^{(e)}. \quad (27)$$

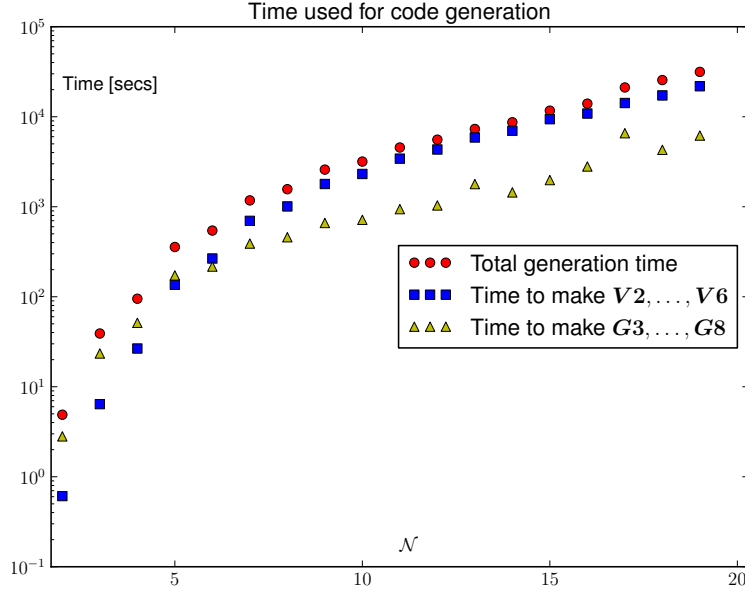


Figure 7: This figure illustrates how the time used for code generation scale with system size \mathcal{N} for the Hamiltonian (26). When \mathcal{N} is large the most time-consuming individual task seems to be the computation of $\bar{D}_3 V$.

We have generated such Hamiltonians, using a random orthogonal matrix with rational coefficients $R_a^j = R_a^j$, for a range of \mathcal{N} -values (the way we construct R_a^j only nearest- and next-nearest-neighbor couplings are generated between the variables q_j). This allows us to investigate how the code generator behave for models of increasingly size and complexity. As illustrated in Figure 7 the time used to generated the solver module increases quite rapidly with the number \mathcal{N} of variables.

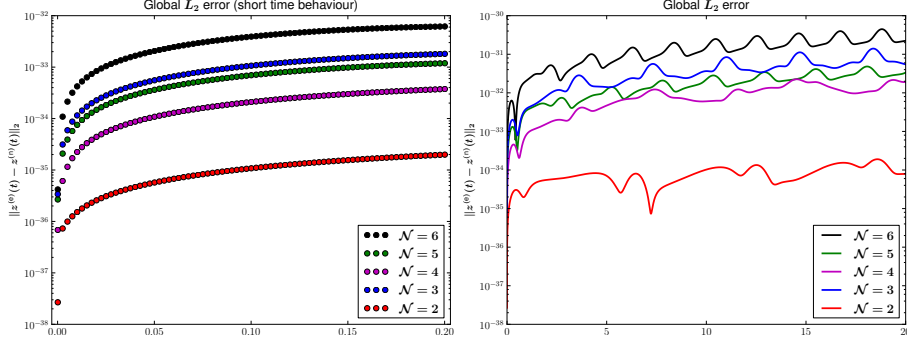


Figure 8: These figures illustrates how the global error varies with time, system size \mathcal{N} , and initial conditions. The short-time behaviour is shown to the left; the long-time behaviour, for the same model and initial conditions, to the right. We have used a multiprecision integrator of order 8, with $\tau = 10^{-3}$ and computations to 35 decimals precision.

In Figure 8 we illustrate how the global error in these models behave. Although there is a general trend that the accuracy deteriorates with system size, this trend is not strictly followed (as can be seen by the case of $\mathcal{N} = 3$). This is a reflection of the fact that both the models and their initial conditions are generated with a certain degree of randomness.

5. Structure of the programs

From a functional point of view our code generating program can be characterized as a *module*, hence it should (to our understanding) be organized into a single file. However, with 1700+ lines of code and comments this would make code development and maintainance impractical. Hence we have organized it as a *package*. I.e., as a set of .py-files, including a file named `__init__.py`, in a directory (folder) with the same name as the module (kimoki). A graphical overview of the main components of this structure is illustrated in Figure 9.

For a given Hamiltonian this module generates one or two *solver modules* with routines for numerical solution of the model, each with a *runfile example* using the solver. Each runfile example is intended to demonstrate and check basic properties of its solver module, and to be modified into more useful programs by the user.

In a separate `examples` directory there is a file named `makeExamples.py`, containing the examples discussed in section 3. By running `makeExamples.py` the examples

directory will, after some time, be populated with several solver modules and runfile examples. Running the runfile examples will in turn generate many .pkl-files with numerical data (which are normally deleted after use), and some .png-files with plots of the solution, and how well the solution respects energy conservation.

5.1. Diagrammatic overview of the code generating module

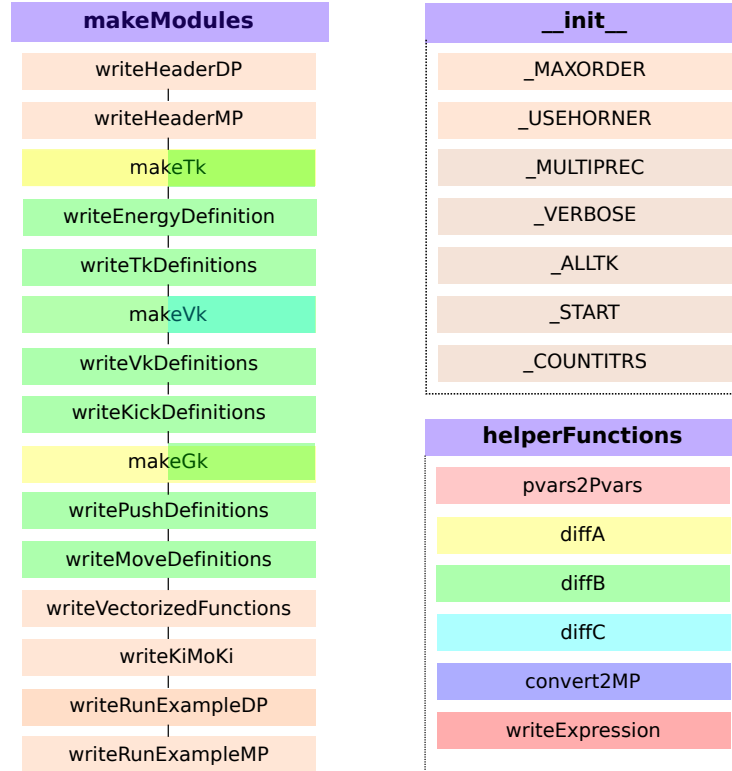


Figure 9: Components of the code generating program. The main process is run in the `makeModules(...)` routine; this calls a sequence of subroutines as illustrated in the left column. This routine takes a number of optional keyword arguments, the values of some of them are stored in global variables (as listed in the `__init__` box). Some functions, most of them required at several places in the program, are collected in `helperFunctions`. All routines listed in the left column, plus `__init__` and `helperFunctions` are defined in files with the same name plus the extension `.py`. These files are in turn collected in the directory (folder) `kimoki`, the name of the code-generating module.

5.2. Brief description of the routines

- `makeModules(modname, V, qvars, pvars[, kwargs])`

This is the main subroutine, and the only one intended to be called by the user. Here `modname` is a “basename” of the generated files, `V` is a symbolic expression

for the potential V , `qvars` is a list of symbolic positions variables (generalized coordinates), and `pvars` is a list of symbolic momentum variables (canonically conjugate momenta). This routine takes a number of optional keyword arguments (`kwargs`) with defaults:

`PARAMS=None` is a list of symbolic parameters used in V .

`MAXORDER=8` is the maximum order of the generated solvers.

`DP=True` is a switch which determines if code for normal (double) precision solvers should be generated.

`MP=False` is a switch which determines if code for multiprecision solvers should be generated.

`VERBOSE=False` is a switch which determines if messages from the code generation process should be written.

`ALLTK=False` is a switch which determines if code for calculating T_2 , T_4 , and T_6 is generated.

`COUNTITRS=False` is a switch which determines if code for monitoring the iterative solution of (9a) is generated. This code makes a histogram of the number of iterations used for solutions.

- `diffA(V, qvars, pvars), diffB(V, V0, qvars), diffC(V, qvars)`

These three functions implement respectively the operator D defined in equation (10), the operator \bar{D} defined in expressions (10), and the operator \bar{D}_3 defined in equation (12). Here $V0$ is a symbolic expression of the potential defining the model, while V can be any symbolic expression depending on `qvars`, `pvars`, and potential parameters `params`. The function `diffA` is used by the routines `makeTk` and `makeGk`; the function `diffB` is used by the routines `makeTk`, `makeVk` and `makeGk`; the function `diffC` is used by the routine `makeVk`.

- `writeExpression(outfile, expression), convert2MP(match)`

The function `writeExpression` writes `expression` to `outfile` in python format. If a multiprecision version of the solver module is generated, the function `convert2MP` is used to assure that fractions are converted to multiprecision format. Optionally a polynomial expression can be converted to Horner form first (this is not recommended if `expression` depends on many variables, due to time and memory use).

- `writeHeaderDP(outfile, pvars, params),`
`writeHeaderMP(outfile, pvars, params)`

These routines write the header part of respectively the double precision and multiprecision solver modules. Some important solver module variables are defined here, with defaults:

`tau = 1/10 (DP), tau = 1/mpf(1000) (MP).`

The timestep τ used by the solvers.

`epsilon = 1/10**12 (DP), epsilon = 1/mpf(10**20) (MP).`

The accuracy to which (9a) must be solved. We have observed that the symplectic preserving property of the solvers is lost when `epsilon` is too large, but it must be somewhat larger than the numerical precision used.

`order = MAXORDER.` Which order of solver to use, setting `order` larger than `maxorder` (see below) has no effect.

`params.` A list of the symbolic potential parameters; these parameters must be set before starting a solution.

`maxorder = MAXORDER.` The maximum order of generated solvers. Must not be changed by the user.

`dim.` The number of phase space variables. Must not be changed.

`itrs[20].` A histogram of how many iterations are used to solve (9a). Exists only if `COUNTITRS` is set to `True`. Must not be changed by the user.

- `makeTk(V0, qvars, pvars)`
Calculates the contributions T_0 , T_2 , T_4 , and T_6 to T_{eff} , cf. (7a), using explicit expressions in (11). T_0 is used by the routine `writeEnergyDefinition`; T_2 , T_4 , and T_6 by the routine `writeTkDefinitions`. T_2 , T_4 , and T_6 are computed only when the optional parameter `ALLTK=True`, otherwise they are set to 0.
- `writeEnergyDefinition(outfile, qvars, pvars, T0, V0)`
Writes the definition of the function `energy(z)`, which evaluates the energy $T_0(\mathbf{p}) + V_0(\mathbf{q})$, cf. equation (2), at the phase space point $z \equiv (\mathbf{q}, \mathbf{p})$.
- `writeTkDefinitions(outfile, qvars, pvars, Tk)`
Writes the definitions of the functions $T_2(z)$, $T_4(z)$ and $T_6(z)$, using the symbolic expressions in the list `Tk` calculated by `makeTk`.
- `makeVk(V0, qvars)`
Calculates the contributions V_2 , V_4 , and V_6 to V_{eff} , cf. equation (7b), using explicit expressions in equation (11). V_2 , V_4 , and V_6 are used by the routines `writeVkDefinitions` and `writeKickDefinitions`.
- `writeVkDefinitions(outfile, qvars, Vk)`
Writes the definitions of the functions $V_2(\mathbf{q})$, $V_4(\mathbf{q})$ and $V_6(\mathbf{q})$, using the symbolic expressions in the list `Vk` calculated by `makeVk`.
- `writeKickDefinitions(outfile, qvars, Vk)`
Calculates the symbolic expressions $-\partial V_{\text{eff}}/\partial q^a$, cf. equation (3), using symbolic expressions in the list `Vk` calculated by `makeVk`. These expressions are used to define the functions `kicka(z)` used in the *kick*-steps of the solvers.
- `makeGk(V0, qvars, Pvars)`
Calculates the contributions G_3, G_4, \dots, G_8 to the generation function $G(\mathbf{q}, \mathbf{P}; \tau)$, cf. equation (8), using the explicit expressions in equation (13). G_3, G_4, \dots, G_8 are used by `writePushDefinitions` and `writeMoveDefinitions`.

- `writePushDefinitions(outfile, qvars, Pvars, Gk)`
Calculates the symbolic expressions $\partial G/\partial q^a$, cf. equation (9a), using symbolic expressions in the list `Gk` calculated by `makeGk`. These expressions are used to define the functions `pusha(z)` used in the *push*-steps of the solvers.
- `writeMoveDefinitions(outfile, qvars, Pvars, Gk)`
Calculates the symbolic expressions $\partial G/\partial P_a$, cf. equation (9b), using symbolic expressions in the list `Gk` calculated by `makeGk`. These expressions are used to define the functions `movea(z)` used in the *move*-steps of the solver(s).
- `writeVectorizedDefinitions(outfile, qvars, Pvars)`
Writes definitions of functions `vecKicks(idx, z)`, `vecPushes(idx, z)`, and `vecMoves(idx, z)`, *simulating* parallel evaluation of `kicka(z)`, `pusha(z)`, and `movea(z)`, for all a in the list `idx`. We don't think parallel evaluation is actually achieved⁴; hence presently this is only *syntactic sugar* simplifying the main solver routine, `kiMoKi(z)`.
- `writeKiMoKi(outfile)`
Writes the definition of the main algorithm of the solver module, `kiMoKi(z)`. The routine `kiMoKi(z)` processes the *kick-push-move-kick* substeps of a full timestep, including the iterative solution of equation (9a).
- `writeRunExampleDP(outfile, modname, qvars, pvars, params)`,
`writeRunExampleMP(outfile, modname, qvars, pvars, params)`
Writes a simple example program illustrating how to use the solver module. Some routines of this program solves the Hamilton's equation over a time interval, with random initial conditions and parameters (which most likely must first be manually changed to sensible values), and writes a plot of the solution to a pdf file. Other routines check how well energy is conserved by the solver, for a set of timesteps, and writes a plot of the energy errors to another pdf file.

⁴This depends on how the `numpy.vectorize` function is implemented.

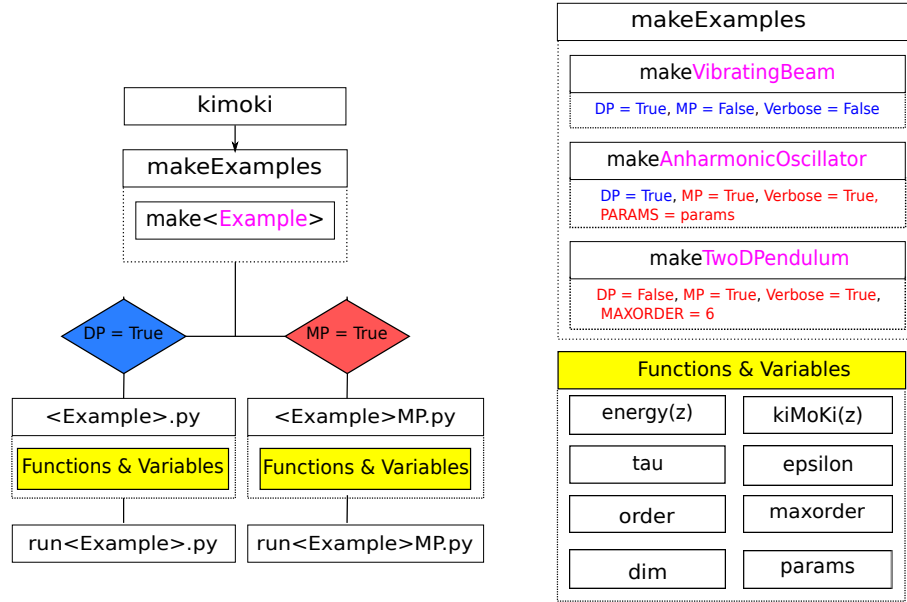


Figure 10: This figure illustrates use of the code generator. The call of `kimoki.makeModules('<Example>',...)` will generate a solver module, `<Example>.py`, and a demonstration runfile `run<Example>.py`. When the optional parameter `MP=True` a multiprecision version of the solver module and runfile is generated. The solver module consists of various functions and variables. Its most important function is `kiMoKi(z)`, which updates the solution `z` through one full timestep. The function `energy(z)` evaluates the Hamiltonian at the phase space point `z`. Many other functions are also defined. F.i., `T2(z)`, `T4(z)`, `T6(z)` (these return 0 if `ALLTK=False`), and `V2(z)`, `V4(z)`, `V6(z)`. Plus additional functions which are not intended to be called directly by the user. Several parameters, some which can be changed by the user, are also defined: The timestep `tau`, the accuracy `epsilon` to which equation (9a) must be solved, which order of the integrator to use when running `kiMoKi(z)`. The maximum order `maxorder` of solvers available (must not be changed by the user), the phase space dimension `dim` of the model being solved (must not be changed by the user), and a (possibly empty) list of parameters `params` on which the Hamiltonian depends (must not be changed by the user).

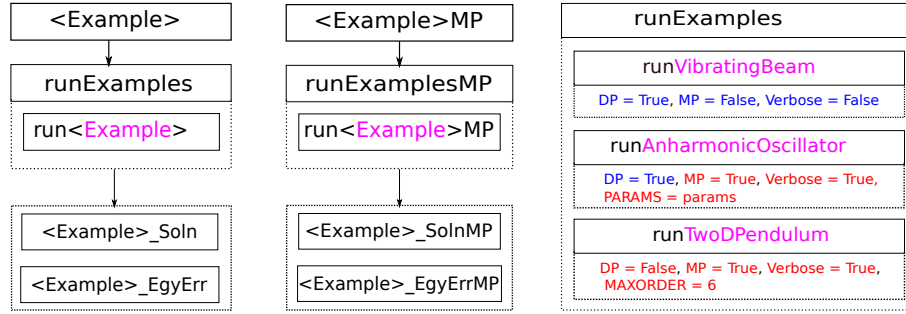


Figure 11: This figure illustrates the runfile example. Normally the runfile generates two figure files in .png format (this can easily be changed to .pdf format by the user). The runfile also generate several intermediate files. Their names begin with the symbol #. These files are normally deleted after use (this can easily be changed by the user).

6. Concluding remarks

In this paper we have demonstrated that the proposed extensions of the standard Störmer-Verlet symplectic integration scheme can be implemented numerically, and that the implemented code behave as expected with respect to accuracy. Here we have not focused on time or memory efficiency of the generated code, which may be viewed as a reference implementation known to work correctly. We have experienced this to be a good starting point for manual implementation of more efficient code for large, structured systems, f.i. the Fermi-Pasta-Ulam-Tsingou type lattice models studied in [9], and molecular dynamics type simulations studied in [12]. Code for the latter systems are quite straightforward to implement using NumPy arrays [13], which also leads to efficient working code.

It is also straightforward to modify our program to generate code in other computer languages.

Acknowledgements

We thank professor Anne Kværnø for useful discussions, helpful feedbacks, and careful proofreading. We also acknowledge support provided by Statoil via Roger Sollie, through a professor II grant in Applied mathematical physics.

References

- [1] J. M. Sanz-Serna, M. P. Calvo, *Numerical Hamiltonian Problems*, Chapman and Hall, (1994)
- [2] R. I. McLachlan, G. R. Quispel, *Splitting methods*, Acta Numerica, 341–434 (2002)

- [3] E. Hairer, Ch. Lubich, G. Wanner, *Geometric Numerical Integrators. Structure-Preserving Algorithms for Ordinary Differential Equations*, Springer-Verlag, 2nd edition (2006).
- [4] I. Newton, *Philosophiæ Naturalis Principia Mathematica* (1687).
- [5] Richard Feynman, *The Character of Physical Law*, p. 43, Penguin Science series, Penguin Books, London (1992).
- [6] C. Störmer, *Méthode d'intégration numérique des équations différentielles ordinaires*, C.R. Congress Internat. Stassbourg 1920, 243–257 (1921).
- [7] Loup Verlet, *Computer “Experiments” on Classical Fluids. I. Thermodynamical Properties of Lennard-Jones Molecules*, *Physical Review* **159**, 98–103 (1967).
- [8] H. Goldstein, *Classical Mechanics* (3rd ed.), Addison-Wesley, 589–598 (2001).
- [9] A. Mushtaq, A. Kværnø, K. Olaussen, *Higher order Geometric Integrators for a class of Hamiltonian systems*, *International Journal of Geometric Methods in Modern Physics*, **11**, 1450009-1–1450009-20 (2014). DOI: 10.1142/S0219887814500091, [arXiv.org:1301.7736](https://arxiv.org/abs/1301.7736)
- [10] A. Mushtaq, A. Kværnø, K. Olaussen, *Systematic Improvement of Splitting Methods for the Hamilton Equations*, *Proceedings for the World Congress on Engineering*, London July 4–6, Vol I, 247–251, (2012). [arXiv.org:1204.4117v1](https://arxiv.org/abs/1204.4117v1).
- [11] M. Abramowitz and I.S. Segun, *Handbook of Mathematical Functions*, Ch. 16, Dover Publications (1968)
- [12] A. Mushtaq, A. Noreen, K. Olaussen, and R. Sollie, *Ensemble and Occupation Time Probabilities, and the Rôle of Identical Particles*, in preparation (2013).
- [13] S. van der Walt, S.C. Colbert, G. Varoquaux, *The NumPy Array: A Structure for Efficient Numerical Computation*, *Computing in Science & Engineering* **13**, 22–30 (2011).